Journal of Hazardous Materials 168 (2009) 484–492

Contents lists available at ScienceDirect

Journal of Hazardous Materials

journal homepage: www.elsevier.com/locate/jhazmat

Visible light degradation of Orange II using xCu_yO_z/TiO_2 heterojunctions

N. Helaïli [a], Y. Bessekhouad [a,b,*], A. Bouguelia [a], M. Trari [a]

[a] Laboratory of Storage and Valorization of Renewable Energies, Faculty of Chemistry, U.S.T.H.B., BP 32, 16111, El-Alia, Algiers, Algeria
[b] National Veterinary School, BP 161-El Harrach, Algiers, Algeria

ARTICLE INFO

Article history:
Received 30 October 2008
Received in revised form 17 January 2009
Accepted 10 February 2009
Available online 23 February 2009

Keywords:
Heterojunctions
Narrow band gap
IPEI
Photocatalytic degradation

ABSTRACT

Cu_2O/TiO_2, $Cu/Cu_2O/TiO_2$ and $Cu/Cu_2O/CuO/TiO_2$ heterojunctions were prepared and studied for their potential application as photocatalysts able to induce high performance under visible light. Orange II was used as a representative dye molecule. The effect of the amount and composition of the photosensitizers toward the activation of TiO_2 was studied. In each case, the global mechanism of Inter Particle Electrons Injection (IPEI) was discussed. The highest photocatalytic activity was observed for the system $Cu/Cu_2O/CuO$ (MB2 catalyst) under visible light ($t_{1/2} = 24$ min, $k = 159.7 \times 10^{-3}$ min^{-1}) and for the heterojunction cascade $Cu/Cu_2O/CuO/TiO_2$ (MB2 (50%)/TiO_2) under UV–vis light ($t_{1/2} = 4$ min, $k = 1342 \times 10^{-3}$ min^{-1}). In the last case, the high performance was attributed firstly to the electromotive forces developed under this configuration in which CuO energy bands mediate the electrons transfer from Cu_2O to TiO_2. The formation of monobloc sensitizers also accounts for the decrease of the probability of the charges lost. It was demonstrated that "Cu_2O/CuO" governs the capability of the heterojunction cascade and Cu does not play a significant role regardless of the heterojunction cascade efficiency. The electrical energy consumption per order of magnitude for photocatalytic degradation of Orange II was investigated for some representative catalytic systems. Visible/MB2 and UV/vis MB2 (50%)/TiO_2 exhibited respectively 0.340 and 0.05 kWh m^{-3} demonstrating the high efficiency of the systems.

1. Introduction

In recent years, material science technology focused its attention to develop semiconductors for specific applications [1–3]. One of the most attractive goal concerns the environmental safety and pollution treatment [4–6].

Titanium dioxide "TiO_2" illustrates such type of promising materials used in both power energy production and water treatment. For instance, TiO_2 is able to produce clean hydrogen energy by splitting water under adequate light irradiation [7]. It is also capable to induce advanced oxidation processes under illumination in which organic pollutants can be completely mineralized [8]. TiO_2 exhibits high photoelectrochemical stability. Indeed, their respective energy bands positions are well matched to produce both $O_2^{\bullet -}$ and $OH^{\bullet}$ radicals, respectively from dissolved oxygen and water molecules respectively [9]. However, it has a band gap of 3.2 eV and suffers as a consequence of low solar to chemical conversion efficiencies which do not exceed 1% [10]. The crystalline structure of TiO_2 imposes to the valence band to be of anionic character (made up from O^{2-}: *2p* orbital) and to the conduction band to be of a cationic one (Ti^{4+}: *3d* orbital) [1]. This fact leads the forbidden band to be large and hence unsuitable with respect to the solar light emission spectrum.

Different strategies are commonly used to overcome this drawback such as: doping with transition metals, dye sensitization and Sol–Gel derived TiO_2 nanoparticles [7,2]. The objectives of these modifications are mainly the increase of the photoactivity through respectively the increase of charge carriers concentration to extend the spectral photoresponse to the visible region, and the decrease of the distance traveled by the photoinduced charges to react at TiO_2 surface. It should be considered that the reported strategies aimed to resolve TiO_2 inconveniencies independently, *i.e.* one after the other. However, the results indicate that the cationic doping can also lead to the trap site generations [11]. Organic dyes that act as sensitizers are commonly deteriorated with time and the reduction of the particles size can lead to the appearance of the quantum-size effect which can induce the decrease of the photoactivity [12].

More recently, efforts have been made on the modification of TiO_2 electronic energy bands through an anionic doping process in which atoms with a lower electronegativity than oxygen (such as N, C and S) have been commonly used. Such behavior induces a cathodic shift of the valence band leading to a successful decrease of the band gap energy and meanwhile the conduction band remains unaffected [13–15]. The improvement of the visible light absorption is incontestable. However, the shift of the valence band to the negative value induces a decrease of the electromotive force (e.m.f) that

* Corresponding author at: Faculty of Chemistry, U.S.T.B., BP 32, 16111, El-Alia, Algiers, Algeria. Tel.: +213 70327993; fax: +213 21247311.
E-mail address: ybessekhouad@yahoo.fr (Y. Bessekhouad).

0304-3894/$ – see front matter © 2009 Elsevier B.V. All rights reserved.
doi:10.1016/j.jhazmat.2009.02.066

is considered to be the difference of potential between the valence band of TiO_2 and the redox couple $OH^{\bullet}/H_2O$. Keeping in mind that for unmodified TiO_2, the valence band is still located at +2.53 V_{SHE} and $OH^{\bullet}/H_2O$ at +2.27 V_{SHE} at pH 7 [9]. It is worth mentioning that the kinetic of radicals generation from H_2O is faster than the radicals generation from dissolved O_2 which lead to $O_2^{\bullet -}$. From this point of view, the modification of the valence band property can alter the futures of the conversion efficiency under visible illumination. In addition, the visible light is very weakly absorbed by the anion doped-TiO_2, and is expected to bring only a minor contribution to the photoconvertion efficiency [16].

An alternative way consists to use unmodified TiO_2 in junction with narrow band gap semiconductor (NBG-SC). The latter acts like a photosensitizer under visible light. Such materials are more stable than organic dyes and induce a further e.m.f development. This fact leads to the increasing of the electron transfer kinetic to produce $O_2^{\bullet -}$ radicals. Several works have been devoted to the heterojunctions in which NBG-SCs of various band gaps (from 0.4 to 2.7 eV) were used [17–21]. The heterojunctions were applied to photocatalytic organic pollutant degradation. The experiments were performed under visible as well as UV–vis light. These works focused on the understanding of charge transfer mechanisms and the impact of extending light absorption properties in relation to the photoactivity improvement. Brahimi et al. [17] reported a fundamental study in which a systematic comparison between large panels of heterojunctions has been made. In this study, the difference of the band gaps of the sensitizers and the e.m.fs developed in each configuration were related to the photoactivity to explain the phenomenon taking place. The most important result suggested the existence of critical e.m.f of 0.5 V. Above this value, the heterosystems exhibit a high performance only under visible light. In contrast, for an e.m.f less than 0.5 V, the heterosystems showed a high performance under visible light as well as UV–vis light. However, such heterojunctions are mainly based on Pb, Cd and Bi chalcogenide. These semiconductors are well known to be subject to photocorrosion releasing toxic metals in aqueous media [17,18].

The scope of the present study is to investigate the mechanism of visible light-induced photocatalytic degradation of Orange II assisted by various heterojunctions based on metallic Cu, Cu_2O, CuO and TiO_2. These materials were selected for their respective band energy positions and non toxicity. The effect of the formation of block sensitizers and their qualitative compositions is reported. The observed phenomena were explained according to the photocatalytic activity.

2. Experimental

2.1. Materials

All the reagents used in this work were of analytical grade: Copper Cu powder, ca. 1 μm (Aldrich), Cu_2O powder <5 μm (Aldrich), copper sulphate $CuSO_4{\cdot}5H_2O$ (Riedel-De-Haën AG), D(+)-Glucose $C_6H_{12}O_6{\cdot}H_2O$ (Riedel-De-Haën AG), Hydrazine hydrate N_2H_4 (Aldrich), Sodium hydroxide NaOH (Prolabo), and TiO_2-P25 (Degussa).

2.2. Preparation of the heterojunctions

2.2.1. Simple heterojunction

Copper powder was dispersed in 1 M HNO_3 for 30 s to remove the outer layer of copper and quickly rinsed with distilled water. The cleaned powder was dispersed in a 10^{-3} M $CuSO_4$ solution and boiled for 1 h to obtain Cu_2O layers on the surface of each particle. 1 h of boiling was reported to be an optimum period after which the dissolution of Cu_2O was observed [22], a fact attributed to the increase of the media acidity. This technique allows to obtain Cu/Cu_2O heterosystem. The catalyst obtained from this method is labeled MA2.

2.2.2. Heterojunction of multiple components

With the aim of obtaining a ternary compound two methods has been adopted:

Method b1:

50 ml of $CuSO_4$ (0.3 M) was added to 150 ml of NaOH (1 M) under vigorous stirring. 2.5 ml of N_2H_4 was quickly added to the colloid solution. The obtained mixture was maintained at 60 °C for 2 h. The precipitate was recovered by filtration and subsequently rinsed with distilled water and ethanol.

Method b2:

The same procedure as b1 was repeated except that in this case, 0.075 mol of glucose was added to the solution.

Both the methods b1 and b2 lead to obtain powders constituted by a mixture of Cu, Cu_2O and CuO, *i.e.* multiple heterojunction. The catalysts obtained from the above methods are respectively labeled MB1 and MB2.

All the catalysts were placed in the autoclave filled up to 80 vol% with absolute ethanol, heated at 100 °C for 12 h and cooled slowly to room temperature. The commercial catalyst was also submitted to the hydrothermal process and the resulting catalyst is called MA1.

Pure CuO was obtained by adding a wise drop of 50 ml of $CuSO_4$ (0.3 M) to 150 ml of NaOH (1 M) in presence of PEG (200) at 60 °C for 2 h under vigorous stirring. The mixture was heated at 110 °C overnight and the obtained precipitate was grinded in an agate mortar and subsequently heated at 650 °C for 2 h. After cooling, the powder was homogenized by grinding again followed by further heating at 800 °C for 2 h.

2.3. Experimental techniques

Powder X-ray diffraction (XRD) patterns were recorded on Philips diffractometer equipped with a monochromatized Cu Kα radiation (λ = 1.5405 Å) in the scan range 2θ (20–80°).

Absorption and reflectance spectra of CuO, Cu_2O and TiO_2-P25 were recorded in air at a room temperature with a Cary 500 UV–VIS–NIR spectrophotometer equipped with an integrated sphere. $BaSO_4$ was used as a reference for all measurements. The scan range was from 300 to 1100 nm.

Photocatalytic experiments were performed using a 150 W Philips tungsten–halogen lamp as UV–vis light source placed horizontally to the reactor. The reactor was surrounded by a double walled Borosilicate jacket with water allowing a perfect temperature control. For each experiment, 250 ml of solution was used and 5 ml of aliquot was taken out at regular time intervals. Orange II (10 mg/l) was used as representative organic dye molecule. The catalysts were directly dispersed into the solution and the operating temperature was fixed at 25 °C during the experiment. Samples containing the catalyst were centrifuged prior to analysis with UV–vis spectrophotometer Cary 50 Con. (λ_{max} = 485 nm). When required, UV cutoff filter (poly(methyl methacrylate) (PMMA)) of 10 mm thickness was used.

3. Results and discussion

3.1. Catalysts characterization

Fig. 1 shows the XRD patterns of both commercial and prepared catalyst after hydrothermal treatment. As observed, commercial catalyst modified by hydrothermal process exhibits a pure cuprite

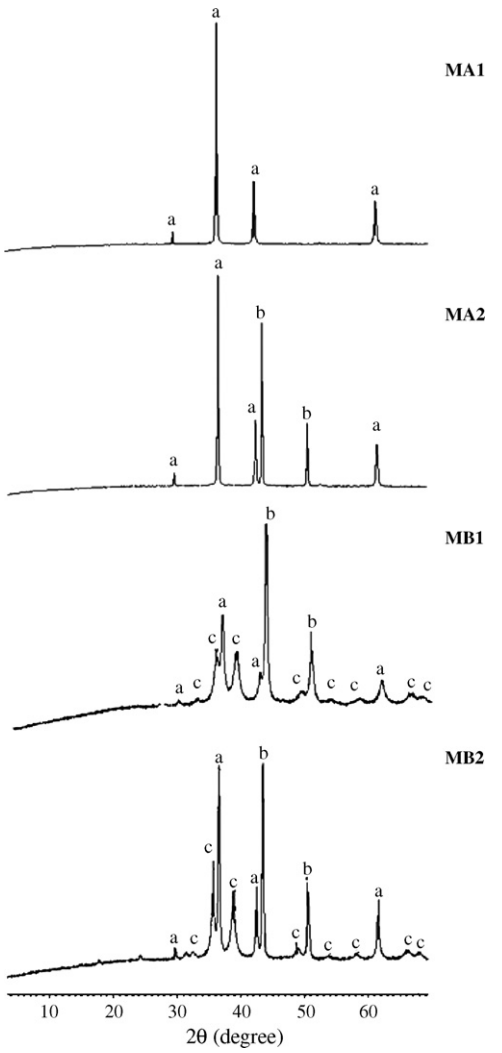

Fig. 1. X-ray diffraction patterns of MA1, MA2, MB1 and MB2 catalysts; (a) Cu_2O, (b) Cu and (c) CuO.

phase and high crystallinity. All the peaks were indexed to a cubic Cu_2O according to the JCPDS file No. 01-078-2076. As expected, the catalyst MA2 was found constituted with metallic Cu (JCPDS-01-070-3039) and well crystallized Cu_2O leading to the constitution of Cu/Cu_2O heterosystem. The catalysts MB1 and MB2 were constituted by a mixture of Cu, Cu_2O and CuO. In addition, the method b2 produced more crystallized particles than b1. The crystallite size of each phase calculated from Scherrer's formula is reported in Table 1.

Table 1
Qualitative composition of the prepared catalyst and the particle size of each phase.

Catalyst	Present phase	L (nm)[a]
MA1	Cu_2O	44
MA2	Cu	47
	Cu_2O	35
MB1	Cu	29
	Cu_2O	24
	CuO	11
MB2	Cu	31
	Cu_2O	39
	CuO	34

[a] L: crystallite size.

The formation of Cu/Cu_2O can be explained by the following chemical reaction:

$$Cu^{2+} + Cu + H_2O \rightarrow Cu_2O + 2H^+ \quad (1)$$

The formation of Cu_2O layer can be limited by two aspects. In the first place, the growth of Cu_2O induce an increase of the media acidity as reported by Fernando et al. [22] leading to the concomitant dissolution of Cu_2O. However, in our opinion the growth limitation of Cu_2O is induced by the formation of Cu_2O layers that act it themselves as a barrier between Cu^{2+} ions and metallic Cu inhibiting the Cu_2O formation.

The general mechanism of the MB1 catalyst formation can be presented as follows:

$$N_2H_4 + 4Cu(OH)_4{}^{2-} \rightarrow 2Cu_2O + N_2 + 6H_2O + 8OH^- \quad (2)$$

Nevertheless, the fact that a mixture of component was obtained, in regard to the XRD analysis, leads to believe that Cu_2O does not result from a one step reaction but through multistep mechanisms. As suggested by Young and Schwartz [23], the processes start first by the reduction of Cu^{2+} to Cu^+ by N_2H_4. This reaction is followed by others which can explain the formation of Cu^0, Cu_2O and CuO:

$$Cu^+ + e^- \rightarrow Cu^0 \quad (3)$$

$$2Cu \rightarrow Cu^0 + Cu^{2+} + 2e^- \quad (4)$$

$$2Cu^+ + 2OH^- \rightarrow 2CuOH \rightarrow Cu_2O \quad (5)$$

$$CuOH \rightarrow CuO + \tfrac{1}{2}H_2 \quad (6)$$

As described, only the reaction (5) leads to the formation of cuprous oxide. In the other cases, the reactions give metallic cupper owing to the strong reduction capability of N_2H_4. Taking into account the results of XRD analysis, it can be suggested that these reactions are certainly concurrent.

When glucose was added to the hydrazine during the preparation, the reduction process is expected to increase. However, the presence of CuO identified by XRD indicates that the same mechanism of particles formation occurs as in the case of pure hydrazine. In our case, this is of a great importance because it permits to obtain particles of multiple components, *i.e.* photosensitizer of metal/SC1/SC2 type, in our case Cu/Cu_2O/CuO.

3.1.1. Optical properties of Cu_2O and CuO

The fundamental absorption, which corresponds to electron excitation from the valence to the conduction band, can be used to determine the nature and the value of the optical band gap (E_g). The relation between the absorption coefficients (α) and the incident photon energy ($h\nu$) varies as [24]:

$$(\alpha h\nu)^{1/n} = C(h\nu - E_g)$$

where C is a constant and the exponent n depends on the type of transition. For direct allowed, $n = 1/2$, for indirect allowed transition, $n = 2$, and for direct forbidden, $n = 3/2$. To determine the possible transitions, $(\alpha h\nu)^{1/n}$ vs. $h\nu$ is plotted for different values of n and the results are shown in Fig. 2. The extrapolation of the linear portion of the plot to the $h\nu$-axis gives the E_g value. Cu_2O exhibits indirect band gap transition of 2.12 eV (Fig. 2a). In contrast, CuO shows a direct band gap transition of 1.35 eV (Fig. 2b). The optical nature of Cu_2O transition is controversial; Rakhshani [25] reported that it is directly allowed. However, our result agrees with that obtained by Khan et al. [26].

3.1.2. The energy band diagram of the antagonist materials

Fig. 3 depicts the potential of the conduction and valence bands for Cu_2O, CuO and TiO_2 at pH 7 (*in non-thermal equilibrium*) along with the HOMO and the LUMO levels of Orange II. Thermodynamic

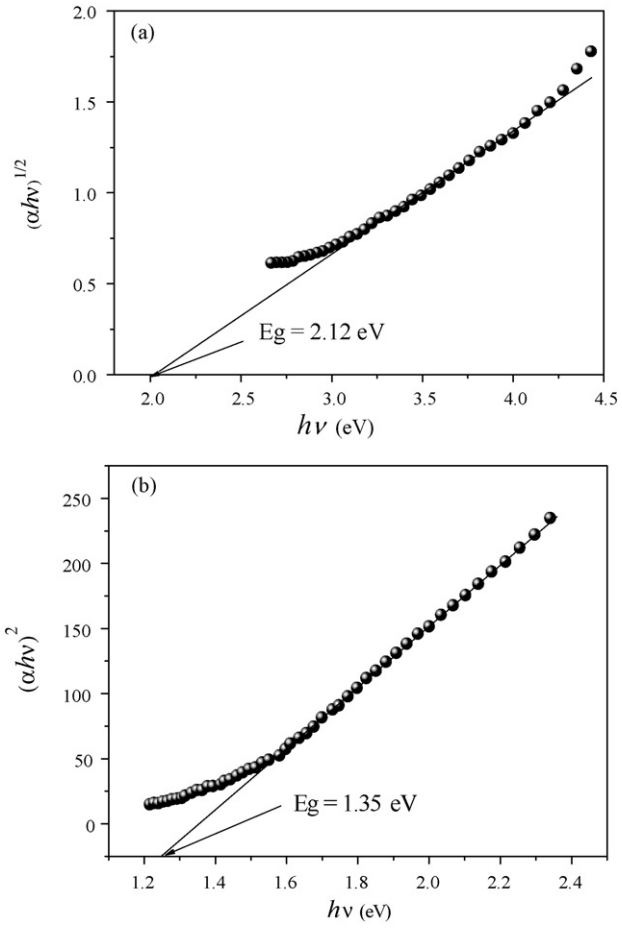

Fig. 2. Optical band gap transition of pure: (a) Cu_2O^i (i: indirect transition) and (b) CuO^d (d: direct transition).

conditions for electron injection to be possible are respected. In fact, the conduction bands of Cu_2O (−1.79 V_{SCE}) and CuO (−1.03 V_{SCE}) are more cathodic than that of TiO_2 [9,28]. This should result in possible electrons transfer leading to consider Cu_2O and CuO as effective candidates for TiO_2 photosensitization when they constitute heterojunctions. The electrons transfer can also take place from Cu_2O to CuO in addition to a possible contribution of Orange II.

3.2. Photocatalytic activity

Fig. 4 shows the normalized absorbances at 485, 310 and 228 nm variation as functions of irradiation time. The selected wavelengths

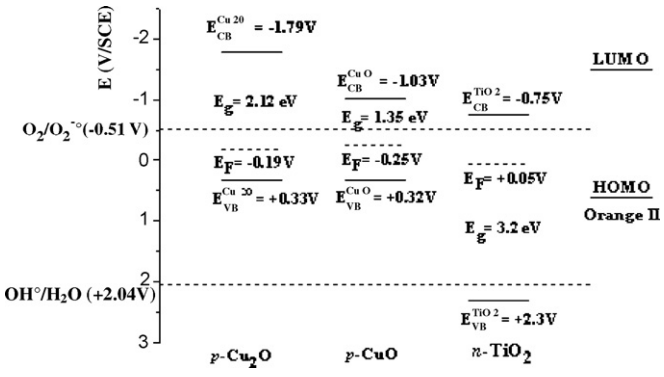

Fig. 3. The energy band diagram of Cu_2O, CuO, TiO_2 and Orange II at pH ∼ 7 in non-thermal equilibrium [9,28].

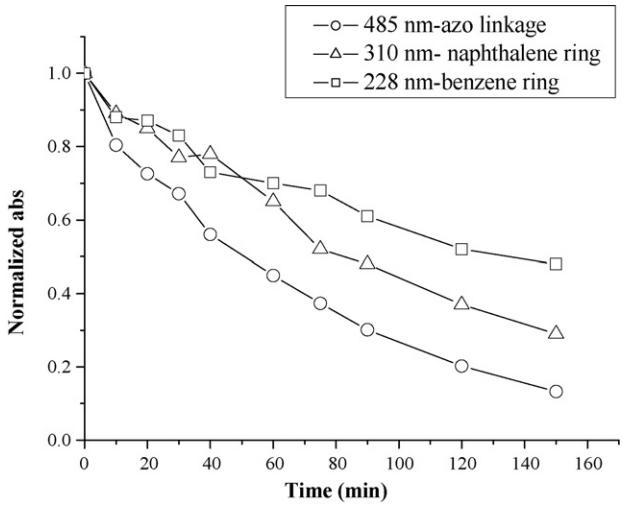

Fig. 4. Normalized absorbances vs. irradiation time of the main UV–vis bands of Orange II in MA1 (50%)/TiO_2 suspension under visible light.

correspond respectively to visible chromophore band (azo-linkage), naphthalene ring and benzene ring absorbance of Orange II [27]. It is observed that the decolorization process take place simultaneously to naphthalene and benzene rings disappearance. In addition, the decolorization rate is higher to that of rings degradation.

OII has not a subject of photolysis and any change in OII concentration can be attributed only to the heterogeneous photocatalysis. Photodegradation experiments of OII by catalysts process exhibited pseudo-first-order kinetics with respect to the concentration of the organic compound

$$-\mathrm{d[OII]}/\mathrm{d}t = k_{obs}[\mathrm{OII}]$$

whose integration gives, for $[\mathrm{OII}] = [\mathrm{OII}]_0$ at $t = 0$:

$$\ln\left(\frac{[\mathrm{OII}]_0}{[\mathrm{OII}]}\right) = k_{obs}t$$

the photoactivity can then be expressed in terms of the half-life of OII. This behavior is in good agreement with that observed by Stylidi et al. [27]. It should be considered that the first-order kinetic indicates that the photoactivity is limited by the diffusion of the pollutant to catalyst active sites in which the radicals are generated. The curve follows an apparent exponential law.

3.2.1. Effect of the sensitizer concentration

The study of the effect of sensitizers on the activation of TiO_2 under both visible and UV–vis light was performed by varying the mass of sensitizers while keeping the mass of TiO_2 (125 mg) constant. We report in Figs. 5 and 6 this variation as a percentage of sensitizers with respect to the total mass of catalyst. Note that electrons transfer take place during collisions between particles [21].

3.2.1.1. Under visible light. Degradation of OII under visible light using pure TiO_2 has not been observed. This result is in agreement with that observed earlier [18,19] and can be attributed firstly to the non activation of TiO_2 under visible light and secondly, to the very low adsorption of the dye. In the last case, electron injection from LUMO of OII to the conduction band of TiO_2 cannot occur. In contrast, all the heterojunctions showed visible light activation even for low concentrations on the sensitizer (Fig. 5). Indeed, the efficiency of the composite materials increases with the increase of the photosensitizer amount. Such behaviors can be reasonably attributed firstly to the increase of visible light harvesting particles and secondly to the increase of the probability of particles collision which favors electrons transfer. Note that up to critical concentrations,

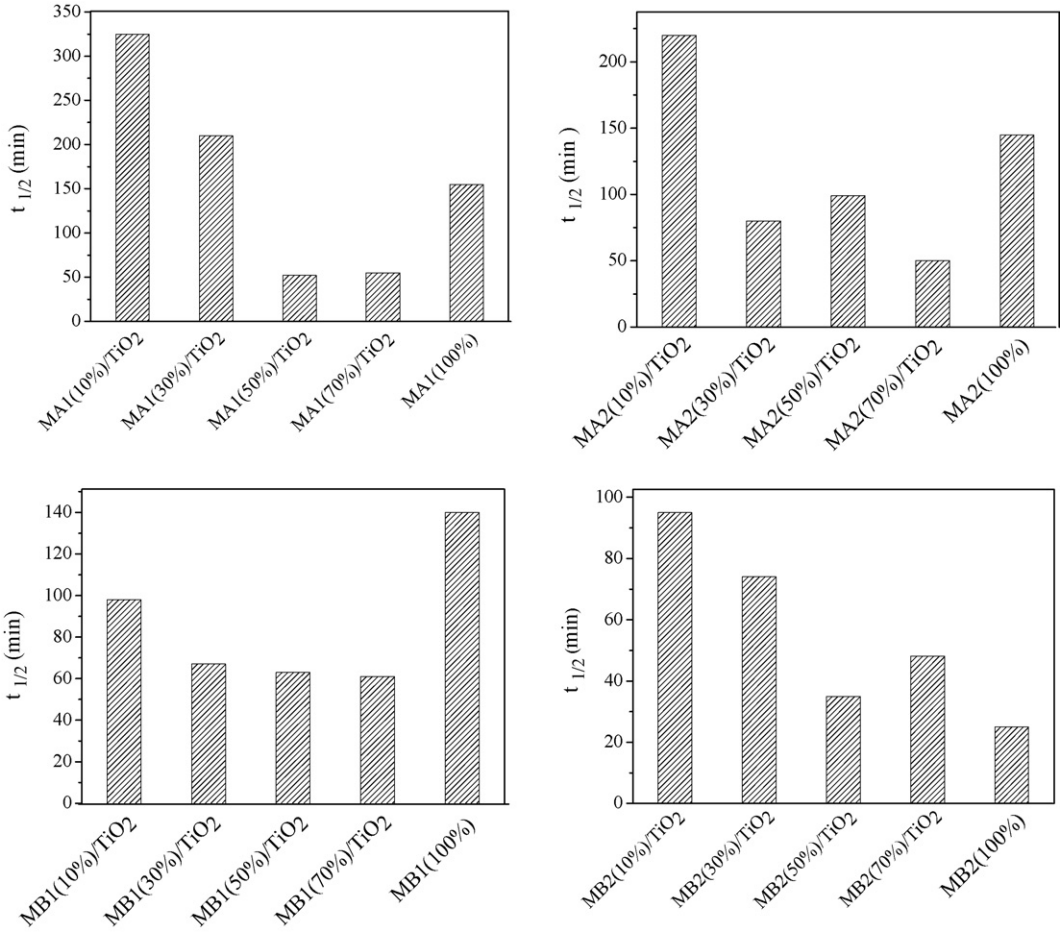

Fig. 5. Effect of the sensitizers concentration toward the photocatalytic activity of TiO_2 based heterojunctions under visible light. Experimental conditions: Orange II initial concentration: 10 mg l^{-1}, volume of the solution: 250 ml, light source: tungsten–halogen lamp of 150 W equipped with PMMA filter, initial pH ~ 6.4.

a decrease and/or stabilization of the efficiencies were observed. The optimum configurations are MA1 (50%)/TiO_2, MA2 (70%)/TiO_2, MB1 (30%)/TiO_2 and MB2 (50%)/TiO_2. The optimum compositions depend strongly on the nature of the photosensitizer.

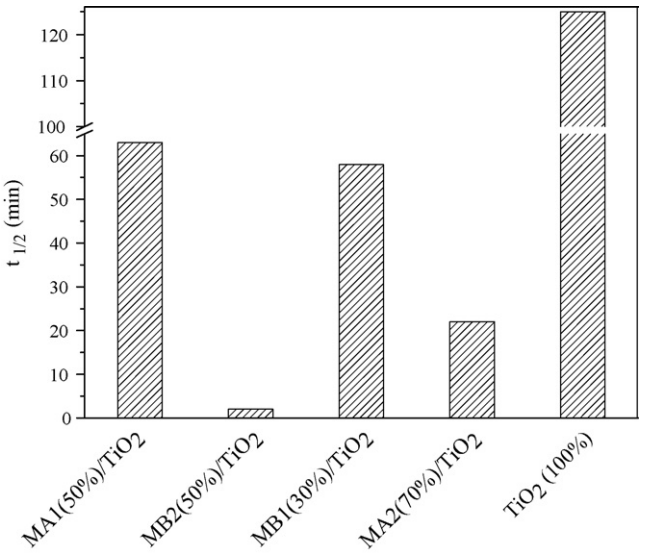

Fig. 6. Photocatalytic activity of the best heterojunctions under UV–vis light. Experimental conditions: Orange II initial concentration: 10 mg l^{-1}, volume of the solution: 250 ml, light source: tungsten–halogen lamp of 150 W, initial pH ~ 6.4.

The comparison between the photoactivities of the prepared catalysts (TiO_2 free) suggests that the composition of each one plays an important role toward the efficiency. This is illustrated by the fact that the catalysts of multiple components are more efficient than the catalyst of simple constituent, *i.e.* MA1 and MA2. In addition, the catalyst MB2 exhibits a very high activity ($t_{1/2}$ of 24 min) indicating the superiority of cascade heterojunctions. This degradation rate is greater than all the TiO_2 based heterojunctions bearing in mind that MB2 is constituted by Cu/Cu_2O/CuO. It should be considered at this stage that though MB1 and MB2 have the same qualitative composition, *i.e.* constituted by Cu_2O, CuO and Cu, their photoactivities are different. This fact can be attributed to the difference of quantities of each species which is corroborated by the difference of the intensity of the pics and the crystallite sizes of each phase (see Fig. 1 and Table 1). This aspect will be discussed below. If we compare between MB2 alone and MB2 (50%)/TiO_2 in which the same amount on MB2 was used, we observe a decrease of the photoactivity. This behavior leads to believe that in this case TiO_2 induces a dissipation of the created charges.

3.2.1.2. Under UV–vis light. The efficiency of the best heterojunction was studied under UV–vis light (Fig. 6). Except for MA1 (50%)/TiO_2, all the heterojunctions showed an increase of their photoactivity. MB2 (50%)/TiO_2 which was less efficient than MB2 alone becomes more efficient under UV–vis light. 50% of OII concentration was removed after less than 4 min of irradiation. This time is 9 and 6 times lower than that observed under visible light and using MB2

Table 2
The composition effect toward the photoactivity of the heterojunctions.

Number	Cu (mg)	Cu_2O (mg)	CuO (mg)	TiO_2 (mg)	$t_{1/2}$ (min)	k (min^{-1})
1	13.88	–	–	125	545	0.011
2	125	–	–	125	138	0.037
3	–	125	125	125	136	0.044
4	–	125	13.88	125	43	0.116
5	–	125	13.88	–	71	0.056
6	–	125	125	–	1000	0.005
7	13.88	125	13.88	–	70	0.050
8	13.88	125	13.88	125	83	0.049
9	125	125	13.88	125	111	0.026

alone. This fact indicates once more the efficient superiority of the heterojunctions of multiple components. Pure TiO_2 showed a usual activity under UV–vis light but remained very poor in comparison to the heterojunctions. The decrease of MA1 (50%)/TiO_2 activity under UV–vis light is ascribed to the high e.m.f (1.04 V) developed in this configuration which induces thermodynamic control of the efficiency. In this case, when both semiconductors are activated under UV–vis light, the probability of charges lost increase leading to the decrease of the efficiency [17].

3.2.2. Effect of the sensitizers composition

The composition effect toward the photoactivity of the heterojunctions was investigated by studying different heterosystems in which the type and the amount of each species were varied. The photocatalytic experiment was performed under visible light to investigate the sensitization capability. The results of the photoactivity are reported in Table 2.

The first and second configurations indicate that metallic Cu plays a crucial role in the degradation mechanism since the photoactivation of TiO_2 was observed under visible light. However, as it is well known, Cu cannot act as photosensitizer. Nevertheless, Cu mediates the electron injection from OII to the conduction band of TiO_2 making the radical $O_2^{\bullet -}$ generation possible. This idea is comforted by increasing the photoefficiency with increasing Cu amount.

The third and fourth configurations indicate that a suitable TiO_2 photosensitization can be obtained using a small amount of CuO in presence of Cu_2O. This fact was confirmed by the fifth and sixth configurations in which a low amount of CuO induced a high activation of Cu_2O. The activation is only attributed to the heterojunction formation (p-Cu_2O/p-CuO) because CuO alone does not degrade OII. Excess of CuO induces a decrease of the photoactivity.

The eighth and ninth configurations indicate that in the case of heterojunction cascade formed by Cu_2O/CuO/TiO_2, the addition of Cu does not improve the performance and this whatever their amount. This fact can be attributed to the efficiency of the Cu_2O/CuO which was not improved in presence of Cu "seventh configuration". At this stage, the overall results suggest the following conclusions:

- Metal Cu can act as a bridge which permits electrons transfer from non adsorbed dye to TiO_2 leading to the photosensitization to be possible.
- p-Cu_2O/p-CuO is the dominant heterojunction that imposes both photosensitization and efficiency of overall systems based on Cu_2O/CuO/TiO_2. For an efficient photoactivity, low CuO concentration and sufficiently high concentration on Cu_2O are requested.
- Cu does not play a significant role in the interparticle electron transfer, *i.e.* between two semiconductors. However, in Cu/SC an improvement of the photoactivity is observed as in the case of the catalyst MB2 (Cu/Cu_2O).

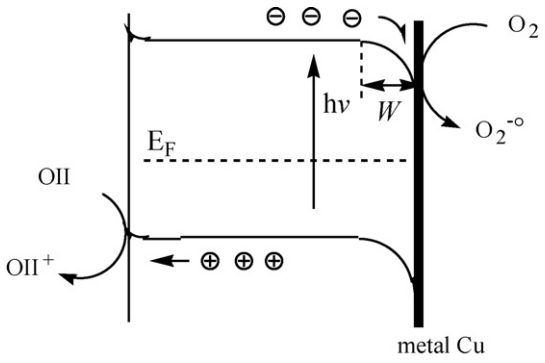

Fig. 7. Schematic presentation of the energy diagram for p-Cu_2O/Cu/Orange II_{aq}.

3.2.3. Discussion of electron transfer mechanism

The processes which take place in different heterojunction configurations are illustrated in Figs. 7–9. For the Cu/Cu_2O heterosystem, incident energy greater than 2.12 eV leads to electrons excitation from the valence band to the conduction one. The pairs (e^-/h^+) are separated by the electric field developed across the depletion layer (W) and migrate toward the surface to react with the species present in the electrolyte. These behaviors are attempted to happen using Cu/Cu_2O because only Cu_2O is subjected to photoexcitation. However, according to the results of the photoactivity in

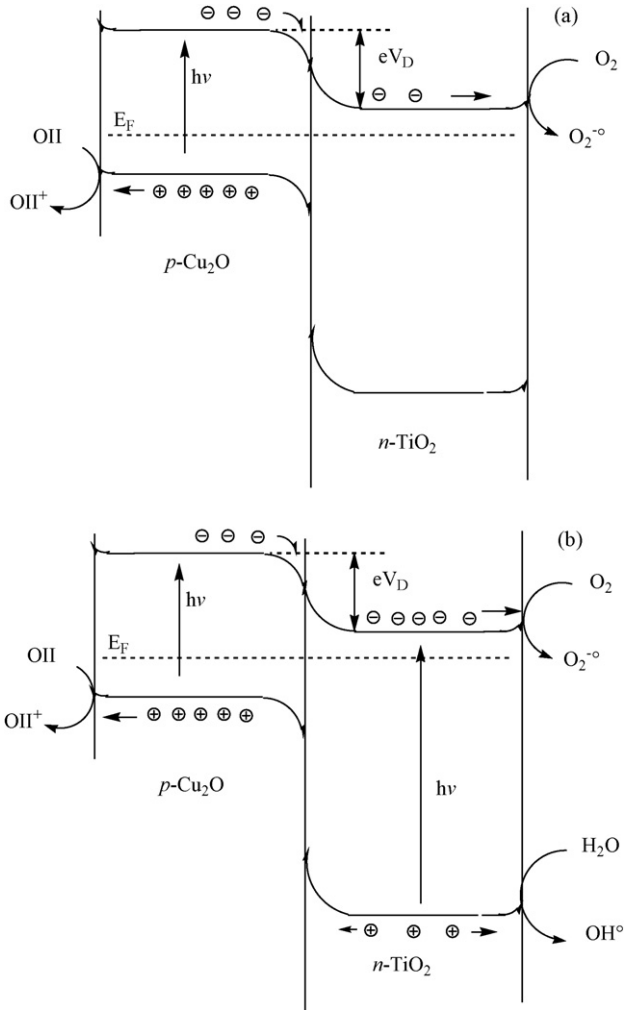

Fig. 8. Schematic presentation of the energy diagram (*in thermal equilibrium*) for a p-Cu_2O/n-TiO_2/Orange II_{aq} configuration under: (a) vis light, (b) UV–vis light.

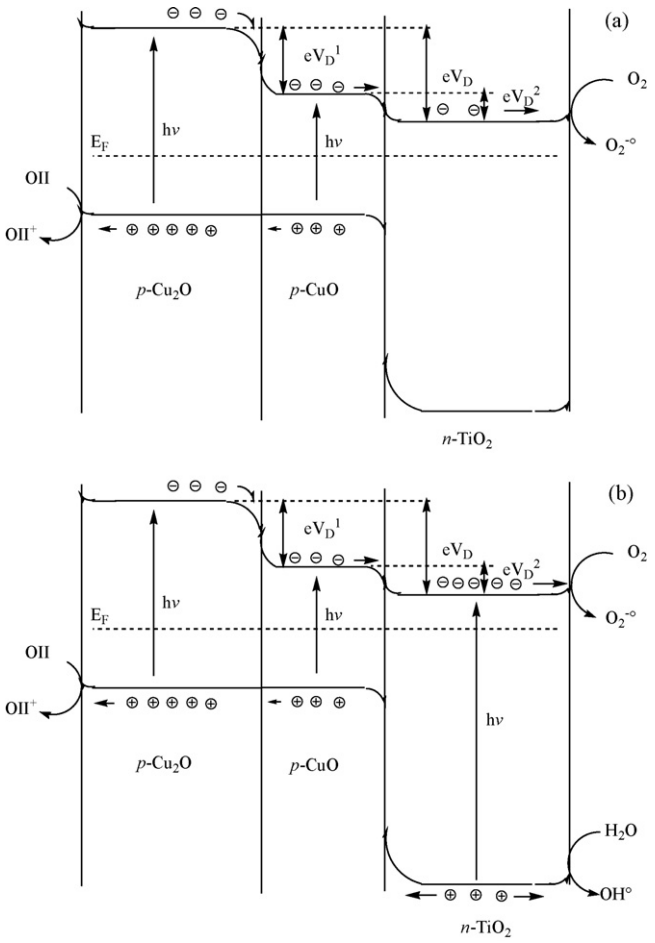

Fig. 9. Schematic presentation of the energy diagram (*in thermal equilibrium*) for a p-Cu_2O/p-CuO/n-TiO_2/Orange II_{aq} configuration under: (a) vis light, (b) UV–vis light.

which the presence of metallic Cu increases the photoactivity, Cu seems to participate in the global photocatalytic mechanism. It is reasonable to attribute the increasing of the efficiency to the physic developed by the heterosystem Cu/Cu_2O. The high electrical conductivity of Cu compared to that of Cu_2O induces the formation of an apparent ohmic junction. In this regard, Cu produces a fast electrons transfer to the solution inducing radicals generation and the electrons transfer at the interface $Cu–Cu_2O$ can be made without potential drop. In such a case, Cu acts as electron scavenger favoring the charges separation and transfer.

The mechanism of interparticle electron transfer in $Cu/Cu_2O/TiO_2$ and Cu_2O/TiO_2 heterosystem is closely the same since the presence of Cu with both semiconductors does not show a significant improvement of the efficiency. Detailed mechanism of interparticle electron transfer in the case of Cu_2O/TiO_2 was previously discussed by Bessekhouad et al. [19] taking into account the property of the light sources (visible and/or UV). From a mechanistic point of view, the irradiation of Cu_2O/TiO_2 by visible light induces the activation of Cu_2O which works as photosensitizer (Fig. 8a). The photoelectrons generated in CB-Cu_2O are injected across CB-TiO_2 inducing radicals $O_2^{\bullet -}$ from dissolved O_2. Further charges are generated under UV–vis light due to TiO_2 activation. Keeping in mind the physics of typical p–n junction, when both semiconductors are in contact, thermal equilibrium is obtained with equalization of the Fermi-levels and charges compensation between donors and acceptors of majority carriers resulting in the appearance of diffusion potential (eV_D) [29,30]. The latter is taken as the difference of energy between corresponding conduction bands of each semi-semiconductor ($eV_D = |E_{CB\text{-}TiO_2} - E_{CB\text{-}Cu_2O}| = 1.04\,V$) [29]. This potential plays the role of electromotive force (e.m.f) and favors electrons injection phenomena [30]. Due to electrons localization in such processes in the conduction bands [2,31,32], the efficiency is governed mainly by the band bending and the positions of the conductions band.

Diffusion potential and as a consequence e.m.f induces an increase of the electron transfer rate and improves the charges separation by physical exchange of electrons between antagonist particles. The overall phenomenon leads to an acceleration of the electrons movement and consequently decreases the probability of charges recombination. Such behavior acts as an apparent Schottky type junction in which the interfacial potential barrier is sufficiently low to observe an increase of the efficiency. The existence of high e.m.f makes the Cu effect insignificant.

The discussion presented above was also comforted by the results of Cu_2O/CuO and $Cu/Cu_2O/CuO$ heterojunctions. In these cases, the diffusion potential results from the energy difference between the corresponding conduction bands of the constituents ($eV_D{}^1 = |E_{CB\text{-}CuO} - E_{CB\text{-}Cu_2O}| = 0.76\,V$). The presence of sufficiently high e.m.f leads also to an insignificant role of metal Cu. It should be considered that under visible light, both semiconductors are excited and an accumulation of electrons was obtained in Cu/CuO side leading to the generation of radicals.

Heterojunction cascade is obtained in presence of three semiconductors: Cu_2O, CuO and TiO_2, even with and without metallic Cu (Fig. 9). In such configuration, the electrons are injected from CB-Cu_2O to CB-TiO_2 through CB-CuO. The diffusion potential resulting from the different energy levels is taken as the sum of the energy difference of successive electrons transfer steps and is given by:

$$eV_D = |E_{CB\text{-}Cu_2O} - E_{CB\text{-}CuO}| + |E_{CB\text{-}CuO} - E_{CB\text{-}TiO_2}|$$
$$= 0.76 + 0.28 = 1.04\,V$$

Though, in this case, the diffusion potential has the same value as in the case of Cu_2O/TiO_2; the efficiency of cascade heterojunctions was found the best.

It is important to point out that the appearance of the diffusion potential between two semiconductors leads also to the creation of electrical field (*induced by dipole formation due to the charges compensation*) which inhibits the diffusion and as consequence prevents charges transfer [30]. Taking into account the obtained results, the electron injection across intermediate states of energy has to effect the lowering of the electrical field that prevents charges transfer. In this case, the kinetic improvement of electrons transfer leads to an increase of the photoactivity.

The effect of Cu on the heterojunction cascade was also found in this case insignificant and the enhancement of the efficiency can only be attributed to the photosensitization by the heterojunction "Cu_2O/CuO". In several respects, excess of Cu induces a decrease of the photoactivity probably due to the increase of the catalyst concentration leading to the formation of a screen between the incident light and photoactive particles and/or the light dissipation.

The effect of the contact between particles was observed by comparing the photosensitization of TiO_2 using sensitizers obtained by direct mixture of component with that obtained in situ by chemical synthesis, *i.e.* the case of MB1 and MB2 photosensitizers. As observed, a permanent contact between particles constituting the photosensitiser gives a high photosensitization effect and as a consequence high photocatalytic performance. A permanent contact between particles forming the photosensitizer system ($Cu/Cu_2O/CuO$) induces a permanent electrons transfer and decreases the probability of charges loss before being transferred to TiO_2. This result looks like that obtained for the simple heterojunction CdS/TiO_2 and/or Bi_2S_3/TiO_2 [18,20].

Table 3
Reaction rate constant and EE/O for photodecolorization of OII by representative catalytic systems.

Catalytic system	k_{obs} (min^{-1})	$t_{1/2}$ (min)	P (kW)	EE/O ($kWh\,m^{-3}$)
Visible/MB2[a]	159.7×10^{-3}	24	0.3536×10^{-3}	0.340
UV–vis/TiO_2	44×10^{-3}	127	0.4420×10^{-3}	1.542
UV–vis/MB2 (50%)/TiO_2	1342×10^{-3}	4	0.4420×10^{-3}	0.050

[a] MB2: $Cu/Cu_2O/CuO$.

According to the above discussion the following conclusion must be drawn:

- Metal Cu can improve the photocatalytic activity of single semiconductor by enhancing the kinetic charge transfer due to its high conductivity and in this way a decrease the probability of charges recombination.
- The diffusion potential developed from multiple steps electrons transfer has more impact for improving the efficiency than that developed from one step transition due to the lowering of the electrical field.
- The formation of junction SC/SC suppresses the effect of metal Cu.
- Heterojunction cascade obtained from monobloc of photosensitizers is more efficient than that obtained from direct mixture of semiconductors.

3.2.4. Electrical energy determination

Electrical energy per order (EE/O) is defined as the number of kW h of electrical energy required to reduce the starting pollutant concentration by 1 order of magnitude (90%) in 1 m^3 of contaminated water. The EE/O ($kW\,h\,m^{-3}$) can be obtained from the following equations:

$$EE/O = \frac{P \times t \times 1000}{V \times 60 \times \log(C_i/C_f)}$$

$$\ln\left(\frac{C_i}{C_f}\right) = k_{obs}t$$

where P is the rated power (kW) of the AOP system, t is the irradiation time (min), V is the volume (l) of water in the reactor, C_i and C_f are the initial and final concentrations and k_{obs} is the pseudo-first-order rate constant (min^{-1}) [33,34].

From the equations sited below, EE/O can be obtained as follows:

$$EE/O = \frac{38.4P}{Vk_{obs}}$$

The EE/O values for the photocatalytic decolorization of Orange II by representative catalytic systems are reported in Table 3.

The EE/O values indicated that the prepared heterojuntions are highly efficient in both visible and UV–vis light in regard to the very low electrical energy consumption. This behavior is in good agreement with the kinetic parameters and conveys the high capability of these heterojunctions in comparison to TiO_2. From an economical point of view and taking into account the cost of electricity in Algeria which is 0.1475€ (1.77 Da) per kW h, the contribution to the treatment cost from the electrical energy will be 0.007375€ (0.0885 Da) per m^3.

4. Conclusion

This work aimed at the study the feasibility of extending the optical absorption property of TiO_2 through the use of narrow band gap semiconductors as photosensitizers. The latter is in some cases of simple constituent and in other ones of multiple components but based on Cu^0, Cu^{I+} and Cu^{II+}. The photosensitizers were prepared by chemical reactions and characterized. Their photoefficiencies were investigated under both visible and UV–vis light. The effect of the sensitizers' composition and type of contact between particles were correlated to the photoactivity observed under various configurations. The obtained results suggested the following rules which govern the electrons transfer mechanism: (i) metallic Cu can improve the photocatalytic activity of single semiconductor by the formation of apparent ohmic junction enhancing the charges transfer kinetics; (ii) e.m.f developed from SC/SC heterojunction suppresses the effect of metallic Cu due to the formation of an apparent Schottky type junction; (iii) diffusion potential developed from multiple steps electrons transfer has more impact for improving the efficiency than that developed from one step transition; and (iv) heterojunction cascade obtained from monobloc of photosensitizers is more efficient than that obtained from direct mixture of the semiconductors. The electrical energy consumption per order of magnitude for photocatalytic degradation of OII demonstrates the mean interest to use such systems. This work opens a new opportunity for the use of heterojunction of multiple components of high efficiency under visible light to induce advanced oxidation processes for many environmental applications.

References

[1] U. Diebold, The surface science of titanium dioxide, Surf. Sci. Rep. 48 (5–8) (2003) 53–229.
[2] A.J. Nozik, R. Memming, Physical chemistry of semiconductor—liquid interfaces, J. Phys. Chem. 100 (31) (1996) 13061–13078.
[3] M. Grätzel, Mesoporous oxide junctions and nanostructured solar cells, Curr. Opin. Colloid Interface Sci. 4 (4) (1999) 314–321.
[4] (a) J. Nowotny, T. Bak, M.K. Nowotny, L.R. Sheppard, Titanium dioxide for solar-hydrogen I. Functional properties, Int. J. Hydrogen Energy 32 (14) (2007) 2609–2629;
(b) J. Nowotny, T. Bak, M.K. Nowotny, L.R. Sheppard, Titanium dioxide for solar-hydrogen II. Defect chemistry, Int. J. Hydrogen Energy 32 (14) (2007) 2630–2643;
(c) J. Nowotny, T. Bak, M.K. Nowotny, L.R. Sheppard, Titanium dioxide for solar-hydrogen III. Kinetic effects at elevated temperatures, Int. J. Hydrogen Energy 32 (14) (2007) 2644–2650;
(d) J. Nowotny, T. Bak, M.K. Nowotny, L.R. Sheppard, Titanium dioxide for solar-hydrogen IV. Collective and local factors in photoreactivity, Int. J. Hydrogen Energy 32 (14) (2007) 2651–2659.
[5] S. Günes, N.S. Sariciftci, Hybrid solar cells, Inorg. Chim. Acta 361 (3) (2008) 581–588.
[6] I.K. Konstantinou, T.A. Albanis, TiO_2-assisted photocatalytic degradation of azo dyes in aqueous solution: kinetic and mechanistic investigations: a review, Appl. Catal. B: Environ. 49 (1) (2004) 1–14.
[7] M. Ni, M.K.H. Leung, D.Y.C. Leung, K.A. Sumathy, Review and recent developments in photocatalytic water-splitting using TiO_2 for hydrogen production, Renew. Sust. Energy Rev. 11 (3) (2007) 401–425.
[8] M. Lewandowxki, D.F. Ollis, in: V. Ramamurthy, K.S. Schanke (Eds.), Semiconductor Photochemistry and Photophysics, Basel, New York, 2004.
[9] M. Kaneko, I. Okura, Photocatalysis: Science and Technology, Springer, 2003.
[10] J. Nowotny, C.C. Sorrell, T. Bak, L.R. Sheppard, Solar-hydrogen: unresolved problems in solid-state science, Sol. Energy 78 (5) (2005) 593–602.
[11] Y. Bessekhouad, D. Robert, J.-V. Weber, N. Chaoui, Effect of alkaline-doped TiO_2 on photocatalytic efficiency, J. Photochem. Photobiol., A 167 (1) (2004) 49–57.
[12] X. Li, X. Quan, C. Kutal, Synthesis and photocatalytic properties of quantum confined titanium dioxide nanoparticle, Scripta Mater. 50 (4) (2004) 499–505.
[13] J.L. Gole, J.D. Stout, C. Burda, Y. Lou, X. Chen, Highly efficient formation of visible light tunable TiO_2-xN_x photocatalysts and their transformation at the nanoscale, J. Phys. Chem. B 108 (4) (2004) 1230–1240.
[14] T. Ohno, T. Mitsui, M. Matsumura, Photocatalytic activity of S-doped TiO_2, photocatalyst under visible light, Chem. Lett. 32 (4) (2003) 364–365.
[15] J. Zhao, C. Chen, W. Ma, Photocatalytic degradation of organic pollutants under visible light irradiation, Top. Catal. 35 (3–4) (2005) 269–278.
[16] A.B. Murphy, Band-gap determination from diffuse reflectance measurements of semiconductor films, and application to photoelectrochemical water-splitting, Solar Sol. Energy Mater. Sol. Cells 91 (14) (2007) 1326–1337.

[17] R. Brahimi, Y. Bessekhouad, A. Bouguelia, M. Trari, Improvement of eosin visible light degradation using PbS-sensititized TiO_2, J. Photochem. Photobiol., A 194 (2–3) (2008) 173–180.
[18] Y. Bessekhouad, N. Chaoui, M. Trzpit, N. Ghazzal, D. Robert, J.V. Weber, UV–vis versus visible degradation of Acid Orange II in a coupled CdS/TiO_2 semiconductors suspension, J. Photochem. Photobiol., A 183 (1–2) (2006) 218–224.
[19] Y. Bessekhouad, D. Robert, J.-V. Weber, Photocatalytic activity of Cu_2O/TiO_2, Bi_2O_3/TiO_2 and $ZnMn_2O_4/TiO_2$ heterojunctions, Catal. Today 101 (3–4) (2005) 315–321.
[20] Y. Bessekhouad, D. Robert, J.V. Weber, Bi_2S_3/TiO_2 and CdS/TiO_2 heterojunctions as an available configuration for photocatalytic degradation of organic pollutant, J. Photochem. Photobiol., A 163 (3) (2004) 569–580.
[21] D. Robert, Photosensitization of TiO_2 by M_xO_y and M_xS_y nanoparticles for heterogeneous photocatalysis applications, Catal. Today 122 (1–2) (2007) 20–26.
[22] C.A.N. Fernando, P.H.C. De Silva, S.K. Wethasinha, I.M. Dharmadasa, T. Delsol, M.C. Simmonds, Investigation of n-type Cu_2O layers prepared by a low cost chemical method for use in photo-voltaic thin film solar cells, Renew. Energy 26 (4) (2002) 521–529.
[23] A.P. Young, C.M. Schwartz, Electrical conductivity and thermoelectric power of Cu_2O, J. Phys. Chem. Solids 30 (2) (1969) 249–252.
[24] J.I. Pankove, Optical Processes in Semiconductors, Prentice-Hall Inc., 1997.
[25] A.E. Rakhshani, The role of space-charge-limited-current conduction in evaluation of the electrical properties of thin Cu_2O films, J. Appl. Phys. 69 (4) (1991) 2365–2369.
[26] K.A. Khan, Y.K. Leung, J.F. Kos, Quantum efficiency of Cu_2O electrode in photoelectrochemical cells with and without bias, Renew. Energy 11 (3) (1997) 293–298.
[27] M. Stylidi, D.I. Kondarides, X.E. Verykios, Visible light-induced photocatalytic degradation of Acid Orange 7 in aqueous TiO_2 suspensions, Appl. Catal. B47 (3) (2004) 189–201.
[28] N. Helaïli, Master of Science, University of Science and Technology, Algiers, 2008.
[29] B. Sapoval, C. Hermann, Physics of Semiconductors, Springer-Verlag, 2003.
[30] S.M. Sze, K.K. Ng, Physics of Semiconductor Devices, J. Wiley & Sons, 2007.
[31] O. Khaselev, A. Bansal, J.A. Turner, High-efficiency integrated multijunction photovoltaic/electrolysis systems for hydrogen production, Int. J. Hydrogen Energy 26 (2001) 127–132.
[32] O. Khaselev, J.A. Turner, A monolithic photovoltaic-photoelectrochemical device for hydrogen production via water splitting, Science 280 (1998) 425–427.
[33] S.R. Cater, M.I. Stefan, J.R. Bolton, A. Safarzadeh-Amiri, UV/H_2O_2 treatment of methyl tert-butyl ether in contaminated waters, Environ. Sci. Technol. 34 (4) (2000) 659–662.
[34] J.R. Bolton, K.G. Bircher, W. Tumas, C.A. Tolman, Figures-of-merit for the technical development and application of advanced oxidation technologies for both electric- and solar-driven systems, Pure Appl. Chem. 73 (4) (2001) 627–637.